Role of eelgrass on bed-load transport and sediment resuspension under oscillatory flow

Beatriz Marin-Diaz [1,2] Tjeerd J. Bouma [1,2,3] Eduardo Infantes [1,4]*

[1]Department of Estuarine and Delta Systems, NIOZ Royal Netherlands Institute for Sea Research, Utrecht University, Yerseke, The Netherlands
[2]Groningen Institute for Evolutionary Life Sciences, Community and Conservation Ecology Group, University of Groningen, Groningen, The Netherlands
[3]Department of Physical Geography, Faculty of Geosciences, Utrecht University, Utrecht, The Netherlands
[4]Department of Marine Sciences, University of Gothenburg, Kristineberg, Fiskebäckskil, Sweden

Abstract

Coastal vegetation is widely attributed to stabilize sediment. While most studies focused on how canopy causes flow reduction and thereby affects sediment dynamics, the role of roots and rhizomes on stabilizing the surface sediment has been less well studied. This study aims to quantify interactions between above- and below-ground biomass of eelgrass (i.e., living *Zostera marina* plants and mimics) with surface sediment erosion (i.e., bed load and suspended load), under different hydrodynamic forcing that was created using a wave flume. Belowground biomass played an important role preventing bed-load erosion, by roughly halving the amount of sediment transported after being exposed to maximal orbital velocities of 27 cm s^{-1}, with and without canopy. Surprisingly, for suspended sediment transport, we found opposite effects. In the presence of eelgrass, the critical erosion threshold started at lower velocities than on bare sediment, including sand and mud treatments. Moreover, in muddy systems, such resuspension reduced the light level below the minimum requirement of *Z. marina*. This surprising result for sediment resuspension was ascribed to a too small eelgrass patch for reducing waves but rather showing enhanced turbulence and scouring at meadow edges. Overall, we conclude that the conservation of the existent eelgrass meadows with developed roots and rhizomes is important for the sediment stabilization and the meadow scale should be taken into account to decrease sediment resuspension.

Coastal vegetation provides a broad range of ecosystem services such as nutrient cycling, support for global fisheries, improvement of the water quality, and carbon sequestration (Orth et al. 2006; Gedan et al. 2009; McLeod et al. 2011). In the face of global change, there is a growing interest in the role of mangroves, salt marshes and seagrass meadows in coastal protection (Temmerman et al. 2013; Bouma et al. 2014; Narayan et al. 2016). Coastal protection by vegetation is provided either by the standing biomass and/or by a reduction of the sediment erosion leading to an enhancement of higher foreshores, both related to wave attenuation (Bouma et al. 2014; Möller et al. 2014; Gracia et al. 2018). In this context,

an in-depth mechanistic understanding of the role of coastal vegetation on reducing sediment erosion is pivotal for making predictions in the future, where the frequency and magnitude of extreme sea levels are predicted to increase (Menéndez and Woodworth 2010; Vousdoukas et al. 2018).

Sediment erosion from the surface layer can be caused by the initiation of horizontal sediment transport (i.e., bed load) or by sediment resuspension (i.e., suspended load) (Einstein et al. 1940; Brown et al. 1995). Bed load occurs when sediment particles move along the bottom horizontally by rolling whereas sediment resuspension occurs when the sediment particles are lifted vertically into the water column creating turbidity and reducing the light (Einstein et al. 1940; Brown et al. 1995). Erosion of sediment with grain size smaller than 62.5 μm (mud) can be quantified as turbidity because these sediment particles are carried directly to the suspended load (Aberle et al. 2004). In contrast, sediment with particles larger than 62.5 μm (sand) will have bed-load phase and should not be quantified only as turbidity (Aberle et al. 2004).

Several studies indicate that coastal vegetation may reduce erosion both on bed load form and resuspension (Ward et al. 1984; Christianen et al. 2013; Spencer et al. 2016), which is

*Correspondence: eduardo.infantes@marine.gu.se

normally attributed to a reduction of the hydrodynamics within the canopy (Bos et al. 2007; Infantes et al. 2012; Möller et al. 2014). The reduction of the sediment erosion is important to maintain the water clarity, necessary for seagrass development (Dennison 1987; Duarte 1991), and to retain the sediment in coastal areas (Christianen et al. 2013; Ganthy et al. 2015; Spencer et al. 2016). Whereas a lot of work has focused on the aboveground plant-flow interactions, the effect of belowground biomass (rhizomes and roots) on the sediment stabilization is still relatively poorly studied. The latter is especially true for seagrasses, despite of them being present in many coastal systems.

Reduction of erosion by belowground biomass has been previously assessed in terrestrial and salt-marsh plants (Baets et al. 2009; Feagin et al. 2009 ; Wang et al. 2017). For example, two types of erosion are common in coastal ecosystems: (1) lateral cliff-erosion, which occurs at the front of the (cliffed) salt marsh, or in the edges of vegetation patches, and leads to narrowing of the marsh (Bouma et al. 2009*a*; Lo et al. 2017; Wang et al. 2017), and (2) horizontal surface-erosion, which is the gradual erosion of sediment particles from the surface layer in between the plants, caused by the bed shear stress (Brown et al. 1995; Ganthy et al. 2015). Lateral cliff-erosion of salt marshes seems to be controlled by the sediment type and root biomass at small scale (Feagin et al. 2009; Wang et al. 2017), and is outside the scope of the present study, as we focus on horizontal surface-erosion. In the case of seagrass, rhizomes and roots seem to play a major role in sediment stability (Christianen et al. 2013), but to the best of our knowledge, there are no mechanistic studies that directly quantify the effect of belowground biomass on surface-erosion. Similar to salt-marsh vegetation, we expect the effect of the seagrass belowground biomass on sediment stabilization to interact with other factors as the sediment properties and wave energy (Widdows et al. 2008; Feagin et al. 2009; Wang et al. 2017).

This study aims to (1) quantify how much surface-erosion in the form of both suspended load and bed-load transport are affected by the presence of eelgrass and (2) quantify the relative effect of aboveground and belowground biomass, sediment type, and wave conditions on surface-erosion. To answer these questions, we carried out a flume experiment in which we used both artificial and natural eelgrass on muddy and sandy sediment, by applying a range of wave orbital velocities.

Methods

Eelgrass and sediment collection

Eelgrass samples with intact sediment were collected from the field to keep the sediment properties, aboveground biomass, and belowground biomass undisturbed. Samples were collected in Bokevik bay in the Gullmars Fjord, Sweden (58°14′N, 11°26′E). Sediment with eelgrass was collected between 1.5 and 10 m depth to cover a range of sediment types, eelgrass densities, and morphologies. Samples from 3 to 10 m depth were taken with a

0.35 m × 0.35 m box-core from a vessel and placed into custom-made trays of 0.35 m × 0.35 m (Dahl et al. 2018). The trays with the sediment were transported in PVC boxes to protect the sediment from tilting. Samples from shallow sites (1.5 m) were taken with cores of 12 cm diameter using scuba or snorkeling because the vessel with the box-core could not reach the shallow waters. The sediment thickness collected varied from 5 to 10 cm depending on the sediment compactness. To maintain the plants in optimal conditions until the hydrodynamic experiments, the sediment trays and cores were stored in shallow-water flow through 1500-liter outdoor tanks at the Sven Lovén Centre for Marine Infrastructure, Kristineberg.

Wave flume

The study was conducted in a hydraulic wave flume developed and constructed at the Netherlands Institute for Sea Research (NIOZ) and located at Kristineberg Marine Research Station (Fig. 1a). The wave flume was 3.5 m long, 0.6 m wide, and 0.8 m high (Fig. 1b). Waves were generated with a pneumatic piston and damped with a wave absorber made of synthetic fiber with a slope of 20°. The test section was composed of a PVC box of $0.35 \times 0.35 \times 0.15$ m^3 (length × width × height). The sediment trays were carefully inserted in the test section and adjusted in order to be at the same level as the flume bottom (Fig. 1a). In the case of the samples from shallow sites, five cores were carefully inserted together to fill the test section and one additional core was sliced to fill any remaining gap, producing a continuous bed of minimal disturbed sediment. The flume was filled with seawater until 25 cm depth. For each sediment sample, orbital flow velocities were increased stepwise from 2 to 27 cm s^{-1}, with each time step maintained during 8 min (56 min of wave exposure in total) (Supporting Information Table S1). These conditions represent similar wave exposures in shallow bays where eelgrass is present in the Swedish west coast (Infantes unpubl. data). Waves were measured next to the sample box with a pressure sensor (Druck, PT1830) and sampling rate of 25 Hz. Wave height (*H*) was calculated from the pressure data as,

$$H = 2 * \sqrt{\frac{\sum_{i=0}^{n} P_i^2}{n}} * \sqrt{2} \qquad (1)$$

where *P* is the pressure data.

Flow velocities were measured with an acoustic Doppler velocimeter (ADV) (Nortek, Vectrino) at 10 cm above the bottom and 5 cm in front of the test section to not interfere with the canopy. The sampling rate was 25 Hz, sampling volume of 7 mm, and velocity range of 0.3 m s^{-1}. Mean orbital velocities (U_{rms}, cm s^{-1}) were calculated as,

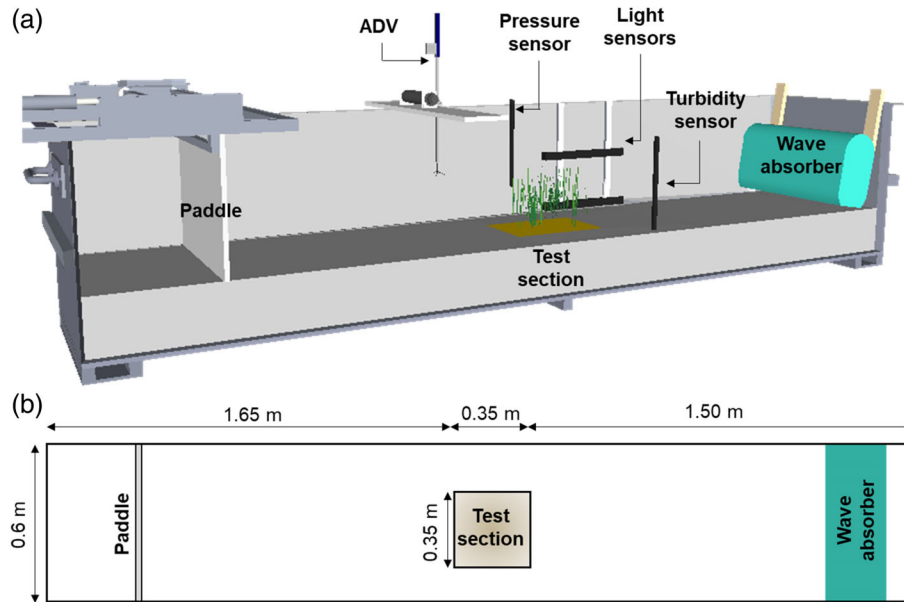$$U_{rms} = \sqrt{\frac{1}{N} \sum_{i=1}^{n} \left(u_i^2 \right)} \qquad (2)$$

Fig. 1. (**a**) Diagram of the hydraulic wave flume and sensors. The wave flume is a further elaboration of the wave mesocosms used by La Nafie et al. (2012) and the wave tanks used by Wang et al. (2017) and (Lo et al. 2017), and (**b**) diagram of the top view of the wave flume. The total length of the flume is 3.5 m, 0.6 m wide, and 0.8 m high.

where u is the horizontal flow velocity during n measurement points.

Suspended load and critical erosion thresholds

Erosion as suspended load and the critical erosion threshold per treatment were assessed by measuring the turbidity and light reduction of the water column. Since sediment type and eelgrass densities varied widely in the field, a first trial with mimic plants aimed to assess the effect of both the absence/presence of shoots, and shoot density on sediment resuspension using the same sediment across treatments. These trials were performed both with muddy and sandy sediment and three treatments (Fig. 2a,b): (1) bare sediment, (2) 40 shoots of mimics in the test section, equivalent to 333 shoots m^{-2}, considered low density, and (3) 90 shoots of mimics in the test section, equivalent to 750 shoots m^{-2}, considered high density (Lefebvre et al. 2010). Mimic shoots were made from four polyethylene blades of 25 cm length, 2 mm width, and 1 mm of thickness attached to a wooden dowel with a 4 cm plastic straw of 0.4 cm of diameter (*see* González-Ortiz et al. 2014). Muddy and sandy sediment was prepared by homogeneously mixing sediment from the field that was previously sieved (2 mm) to remove shells and debris (Table 1).

To quantify the effect of aboveground and belowground vegetation in sediment resuspension in different sediment types, three treatments were made with muddy and sandy intact sediment from the field: (1) eelgrass with both the aboveground and belowground biomass being present; (2) eelgrass from which only the rhizomes and roots were present, by cutting the aboveground leaves; and (3) bare sediment without eelgrass (Fig. 2c,d). Treatment 2 was made only with sandy samples, since pilot trials showed similar results in muddy sediment with eelgrass and only-rhizomes. Three to seven replicates of each treatment were carried out. Hence, our treatments consisted of the test section filled with homogeneous sediment in which we also placed two densities of eelgrass mimics with a random distribution (333 vs. 750 shoots m^{-2}), and natural sediment with either intact eelgrass plants, with eelgrass roots and rhizomes only, and without any eelgrass (Fig. 2).

Water turbidity and the percentage of surface light reaching the bottom were measured during the last 2 min of each time step in all experiments. Water turbidity was measured with a turbidity meter (Campbell, OBS), located 10 cm after the sample box to be in line with the light sensors (Fig. 1a) and 5 cm above the bottom, at a sampling frequency of 25 Hz. At the moment of the measurements, the turbidity was homogeneous in the whole flume. Voltage data from the turbidity meter were calibrated to mg L^{-1} of suspended particles by filtering 0.5 L of water at different concentrations on preweighed filters and calculating the weight difference after drying for 48 h at 60°C. Photosynthetic active radiation (PAR) was measured using two Apogee light meters separated 14 cm for later calculation of the light attenuation coefficients (K_d) and percentage of incident radiation at the bottom (Fig. 1a). Light was generated using two Sirio 2070, 500 W lamps placed 1.1 m above the water surface level. The height of the lamps was chosen in order to provide enough light to the light meter in the bottom. K_d was calculated as,
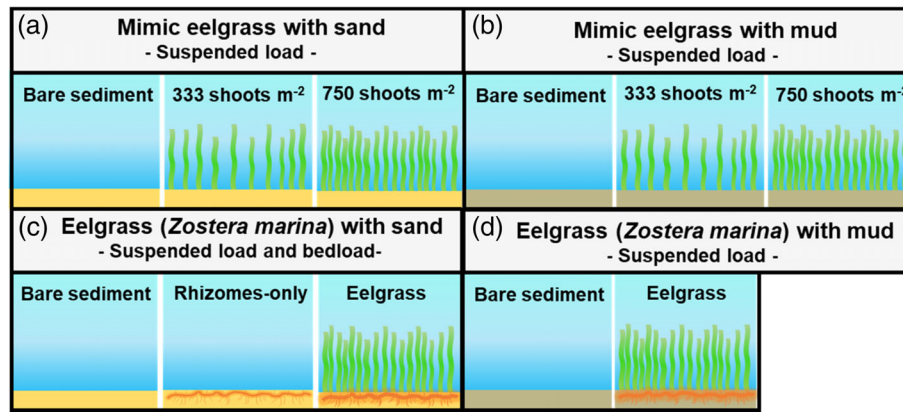
Fig. 2. Experimental design where it was quantified (**a**) suspended load with mimic plants and sandy sediment, (**b**) suspended load with mimic plants and muddy sediment, (**c**) suspended load and bed load with eelgrass and sandy sediment, and (**d**) suspended load with eelgrass and muddy sediment. Treatment "rhizomes-only" includes root and rhizomes biomass.

Table 1. Vegetation and sediment properties, mean (SE).

		Mimic eelgrass		Natural eelgrass	
Number of shoots (in flume)		**Sand**	**Mud**	**Sand**	**Mud**
Seagrass morphology	Number of shoots	—	—	67.1 (8.1)	8.6 (2.4)
	Root diameter (cm)	—	—	0.05 (0.0)	0.07 (0.0)
	Total rhizome length (m)	—	—	6.7 (0.7)	1.4 (0.4)
	Total root length (m)	—	—	71.8 (5.2)	21.1 (5.7)
	Root length density (cm cm^{-3})	—	—	0.8 (0.06)	0.003 (0)
Biomass	DW leaves (g)	—	—	6.1 (1.0)	1.4 (0.1)
	DW rhizomes + roots (g)	—	—	11.1 (0.8)	3.7 (0.8)
Sediment properties	Water content (%)	19.9	59.6	24.1 (0.4)	64.9 (1.94)
	OC (%)	0.4	5.5	0.6 (0.05)	7.4 (0.68)
	Bulk density (g cm^{-3})	1.7	0.6	1.6 (0.03)	0.5 (0.03)
	Sand > 62.5 μm (%)	86.2	3.7	75.8 (3.8)	17.0 (2.2)
	Mud < 62.5 μm (silt + clay) (%)	14.1	96.4	24.2 (3.8)	83.3 (2.2)
	SD$_{50}$ (μm)	256.1	42.1	183.2 (10.9)	53.1 (4.1)

DW, dry weight.

$$K_d = \frac{\ln(I_{z2}/I_{z1})}{Z_2 - Z_1} \qquad (3)$$

where I_{z1} is the PAR irradiance at depth Z_1 and I_{z2} at the deeper depth Z_2 (Beer et al. 2014). The percentage of light at the bottom was calculated as (Beer et al. 2014),

$$\% \text{light at the bottom} = \frac{I_{z2}}{I_{z1}} * 100 \qquad (4)$$

The critical erosion threshold was determined as a measurement of sediment stability. Two erosion phases can be distinguished accordingly to Amos et al. (1992, 1997): a first slow lineal increase of the resuspension with increasing orbital velocities (erosion Type I), and a second rapid increase of resuspension with increasing orbital velocities (erosion Type

II). The first phase may correspond to the resuspension of the organic "fluff" layer (Amos et al. 1992, 1997; Bale et al. 2006). The critical erosions thresholds were determined as the start of the Type II erosion from scattergrams of turbidity plotted against the orbital velocities. The Type II erosion was fitted to an exponential regression where turbidity values below 9.5 mg L^{-1} (ambient concentration) were not accounted.

Bed-load erosion with eelgrass plants

To quantify the role of eelgrass on horizontal sandy sediment transport, bed-load erosion was assessed in sandy samples after the exposition to the seven different wave settings ranging from 0 to 27 cm s^{-1} (Supporting Information Table S1). This experiment was performed with the three sandy treatments (Fig. 2c): (1) eelgrass aboveground and belowground biomass, (2) rhizomes and roots only, and
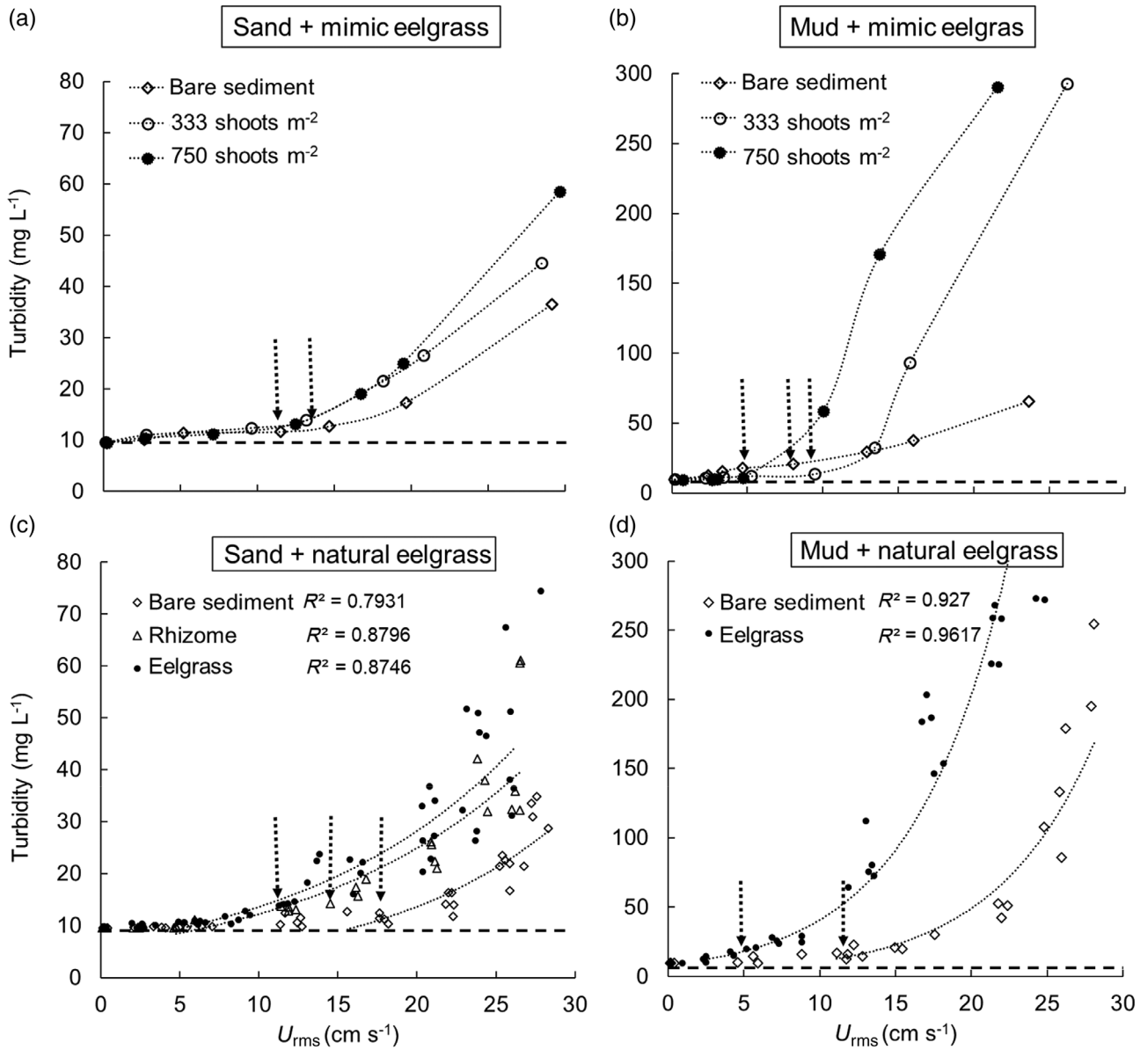
Fig. 3. Orbital flow velocities (U_{rms}, cm s^{-1}) and turbidity (mg L^{-1}) for (**a**) mimic eelgrass with sandy sediment, (**b**) mimic eelgrass with muddy sediment, (**c**) natural eelgrass with sandy sediment, and (**d**) natural eelgrass with muddy sediment. The dashed horizontal line represents the ambient concentration (9.5 mg L^{-1}). The dashed vertical arrows represent the observed critical erosion threshold for eelgrass with sand (12 cm s^{-1}), rhizomes-only with sand (14 cm s^{-1}), bare sand (17.5 cm s^{-1}), eelgrass with mud (4 cm s^{-1}), and bare mud (11 cm s^{-1}), respectively. Each point represents a single measurement. Turbidity against the TKE can be found in Supporting Information Fig. S2.

(3) bare sediment without eelgrass. We defined bed-load erosion as the sediment transported outside of the test-section box. After the trials, the water of the flume was emptied, while the sandy sediment remained on the flume bottom. Then, the sediment deposited on the flume bottom outside of the test-section was collected with a window wiper and a dustpan. The sediment was then dried at 60°C for 1 week and weighed.

Sediment and vegetation properties

Sediment bulk density, organic content (OC), water content, and grain size of the 1–2 cm top layer were determined

for each sample. Bulk density was calculated as sediment dry weight in a volume of 20 mL. Water content was calculated as the difference of wet and dry weight. OC was determined by loss on ignition (LoI) method after burning the sediment sample for 5 h at 450°C. The sediment grain size was analyzed using a Malvern® Mastersizer 2000. Sediment samples with mean grain size above 62.5 μm were classified as sandy, while grain sizes below 62.5 μm were classified as muddy.

Plant morphologies were measured at the end of the experiment for each sample. The length and thickness of the leaves and rhizomes were measured. The *total root length* per sample
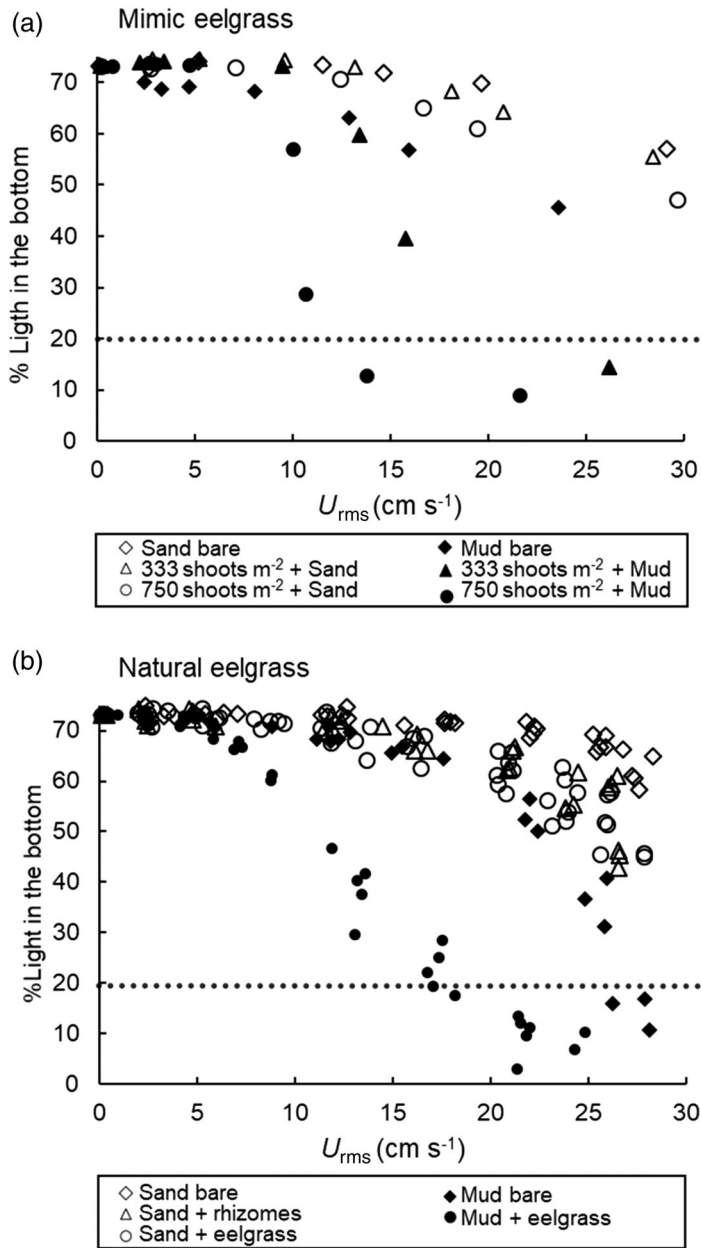
(a)

(b)

Fig. 4. Percentage of surface light reaching the bottom with increasing flow orbital velocities (U_{rms}, cm s^{-1}) for (**a**) mimic eelgrass and (**b**) natural eelgrass. The dot line indicates the minimum light requirement for eelgrass growth (20%).

was extrapolated from the total root biomass of the sample and the dry weight of three subsamples of 15–20 random roots selected from the sample, which were previously measured and then dried at 60°C for 48 h. Then, the diameter of the roots was measured in the subsamples. The *root length density* was calculated using the *total root length* per *volume of sediment* (*see* Baets et al. 2009). Aboveground and belowground biomass were calculated by drying separately the leaves, roots, and rhizomes at 60°C for 48 h.
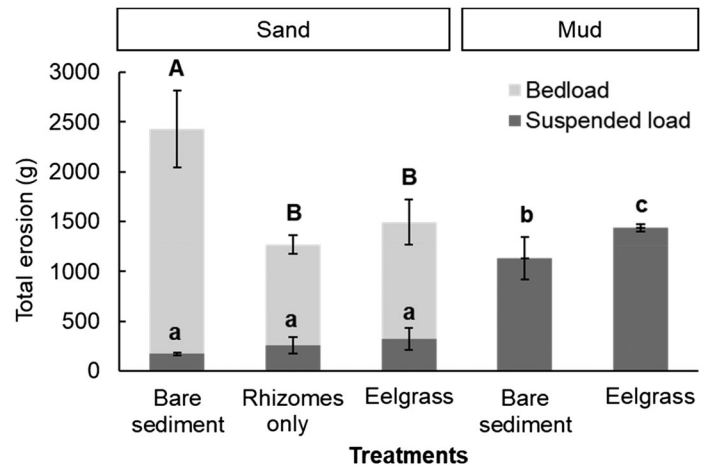

Fig. 5. Total erosion (g) in the form of bed load and suspended load for sandy and muddy trials after 56 min of wave exposure (mean ± SD). Significant differences in the bed load of sandy treatments are indicated by upper case letters and differences in the suspended load between all the treatments are indicated by lower case letters (Tukey HSD, $p < 0.05$). Bed-load erosion in muddy sediment is negligible. Total erosion as suspended load (g) was extrapolated from the turbidity (mg L^{-1}) at the end of the trials to the volume of water contained in the flume, assuming that the turbidity was homogeneous in the whole flume.

Statistical analysis

One-way ANOVAs were used to analyze significant differences in sediment properties, bed-load erosion, and turbidity between the treatments followed by a Tukey's HSD post hoc test. Two-way ANOVA was used to analyze the effect of eelgrass presence and sediment type on turbidity. Differences at p values of 0.05 were considered significant. Turbidity values at 25 cm s^{-1} for each sample were used for the analysis. Spearman correlation coefficients (r_s) and principal component analysis (PCA) (Supporting Information Fig. S1) were done with all the treatments to assess possible correlations between (1) turbidity and plant/sediment characteristics and (2) bed-load erosion and plant/sediment characteristics. Data were standardized for the PCA.

Results

Suspended load and critical erosion thresholds

Sediment resuspension increased at higher densities of eelgrass mimics for both sandy and muddy sediments (Fig. 3a,b). The increase of resuspension was linear during the erosion Type I and exponential during the erosion Type II. After the exposure to all the wave settings, the highest mimic density (750 shoots m^{-2}) reached a maximum turbidity of 58 mg L^{-1} in sandy sediment, while in muddy sediment the turbidity was five times larger, 290 mg L^{-1}. The critical erosion threshold (increase of turbidity and reduction of K_d) started at orbital velocities above 12 cm s^{-1} in sand with eelgrass mimics and at 13.7 cm s^{-1} for bare sand (Fig. 3a). In contrast, the critical erosion threshold started with orbital velocities above 5 cm s^{-1} with 750 shoots m^{-2} and
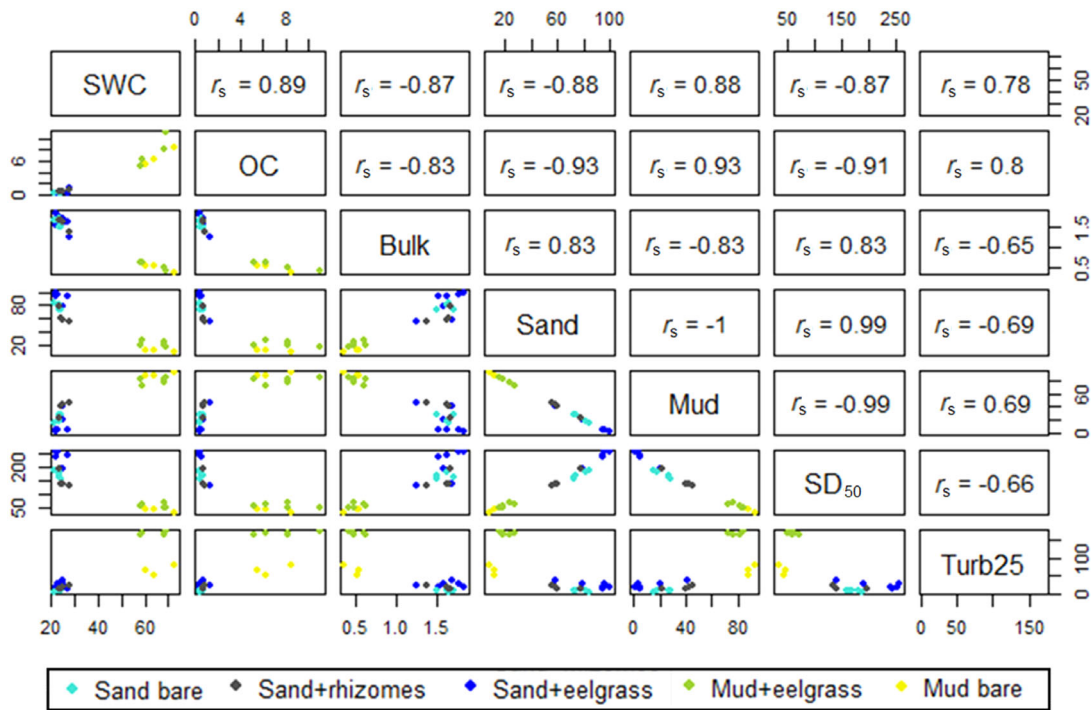
Fig. 6. Matrix plot of the variables significantly correlated with the turbidity. All the Spearman correlation coefficients (r_s) are significant ($p < 0.001$). SWC = sediment water content (%), OC = organic content (%), bulk = bulk density (g cm^{-3}), sand (%), mud (%), SD$_{50}$ = median grain size (μm), Turb25 = turbidity (mg L^{-1}) reached at orbital velocities around 25 cm s^{-1}.

9 cm s^{-1} with 333 shoots m^{-2} in mud with eelgrass mimics (Fig. 3b). The critical erosion threshold in bare mud was lower than with mimics (5 cm s^{-1}), and contrary to the treatments with mimics, turbidity increased linearly at orbital flow velocities above 9 cm s^{-1} (Fig. 3b). The increase in turbidity showed a significant correlation with the light attenuation coefficient (K_d) ($R^2 = 0.97$, $p < 0.001$). The maximum $K_d \approx 3.8$ m^{-1} and ≈ 25 m^{-1} were obtained with sandy and muddy sediment, respectively, at orbital velocities between 21 and 29 cm s^{-1}.

Sediment resuspension in natural samples followed a lineal increase during the erosion Type I and an exponential increase during the erosion Type II in all the treatments (Fig. 3c,d). Critical erosion threshold started at orbital flow velocities around 9.4 cm s^{-1} in sandy sediment with eelgrass, 10.5 cm s^{-1} with rhizomes-only, and at 14.4 cm s^{-1} in bare sediment (Fig. 3c). In contrast, the critical erosion threshold in muddy sediment started at velocities of 5.1 cm s^{-1} in eelgrass samples and 7.6 cm s^{-1} in bare sediment (Fig. 3d). Turbidity and K_d were lower in sandy sediments than in muddy (Fig. 3). K_d reached maximum values of ≈ 3.6 m^{-1} and ≈ 21.4 m^{-1} in sand and mud, respectively, at orbital velocities between 22 and 29 cm s^{-1}. In the muddy trials, rhizomes and roots started to be uprooted around 15 cm s^{-1}, which was not the case in the sandy trials. In addition, the turbulent kinetic energy (TKE) was calculated from the ADV data as a measurement of turbulence, which was correlated to the U_{rms}. Calculations of the TKE and plots of the turbidity with TKE can be found in the Supporting Information Fig. S2.

Eelgrass presence was correlated with higher turbidity in both sandy (Spearman, $r_s = 0.61$, $p < 0.01$) and muddy sediment (Spearman, $r_s = 0.81$, $p < 0.01$). ANOVA and Tukey HSD tested for the turbidity reached at 21 and 25 cm s^{-1} showed significant differences between all the treatments except between rhizomes-only and eelgrass with sand (one-way ANOVA: 21 cm s^{-1}: $F_{2,13} = 14.91$, $p < 0.001$; 25 cm s^{-1}: $F_{2,13} = 11.81$, $p < 0.001$). Given a flume water depth of 25 cm, only the muddy trials reduced the light below the minimum light requirement for *Zostera marina* (20% of surface light) for both mimics and natural eelgrass (Fig. 4). In contrast, none of the sandy trials with or without eelgrass reached the minimum light requirement threshold. In the eelgrass mimics experiment, the light threshold was reached at 10 cm s^{-1} and 15 cm s^{-1} with 750 shoots m^{-2} and 333 shoots m^{-2}, respectively. In natural eelgrass with muddy sediment, the light threshold was reached at orbital velocities of 15 cm s^{-1} with eelgrass and 25 cm s^{-1} with bare sediment (Fig. 4).

Bed-load erosion

Sediment erosion in the form of bed-load transport was significantly lower in the presence of eelgrass and rhizomes-only, when compared to bare sediment (one-way ANOVA: $F_{2,7} = 24.21$, $p < 0.05$) (Fig. 5). The total erosion after 1 h of wave exposure was similar for vegetated sandy sediment, vegetated muddy sediment, and bare muddy sediment, although erosion in sandy trials was mainly as bed load while in muddy trials was mainly as
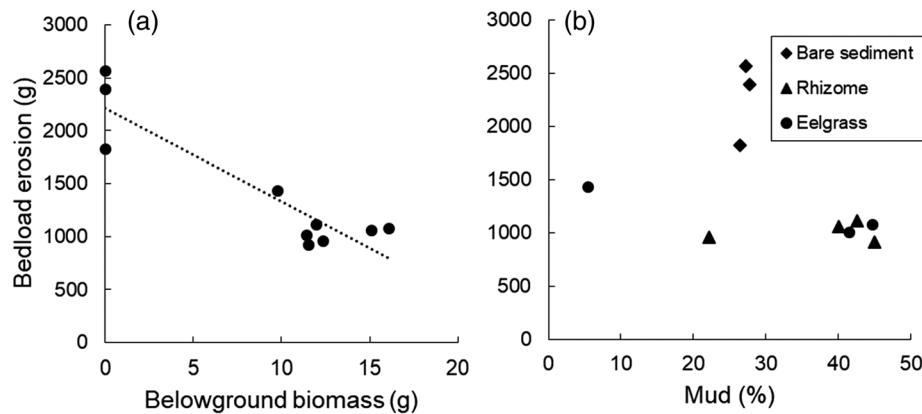
Fig. 7. (**a**) Correlation between belowground biomass (g) and bed-load erosion (g) (Spearman correlation $r_s = -0.68$, $p < 0.001$. (**b**) Scattergram between mud content and bed-load erosion (g). Eelgrass and only-rhizome trials, even with variable mud content, had lower bed-load erosion than bare sediment trials.

suspended load (Fig. 5). In contrast, bare sandy sediment had a predominance of bed-load transport compared to the other treatments (Fig. 5).

Sediment and vegetation properties

Sediment and vegetation properties are summarized in Table 1. The sediment water content and OC were significantly higher in the muddy sediment, whereas the bulk density was significantly higher in sandy sediment (one-way ANOVA: sediment water content: $F_{4,19} = 164.6$, $p < 0.001$; OC: $F_{4,19} = 46.8$, $p < 0.001$; bulk density: $F_{4,19} = 82.09$, $p < 0.001$). No significant differences were found in bulk density, water content, or OC comparing within the sandy or muddy trials separately.

Eelgrass morphology varied between the samples present in sand and mud (Table 1). Leaves were shorter (< 30 cm) and thinner (0.3 cm), rhizomes were thinner (0.25 cm), and root diameter was thinner (0.05 cm) in sandy samples. In contrast, leaves were longer (> 30 cm) and wider (0.7 cm), rhizomes were thicker (0.5 cm), and root diameter was larger (0.07 cm) in muddy samples. In contrast to muddy samples, eelgrass in sandy sediment formed a dense network of roots and rhizomes, which aggregated and retained the sediment.

Water content, OC, and the percentage of mud were significantly correlated to higher turbidity, comparing all the samples (mud and sand) (Fig. 6). Bulk density, the percentage of sand, and the median grain size (SD_{50}) were correlated to lower turbidity (Fig. 6). No significant correlations with plant morphology and turbidity were found. There was a significant interaction between sediment type (mud or sand) and eelgrass presence (two-way ANOVA: $F_{1,19} = 173$, $p < 0.001$), which led to the maximum rates of turbidity and lower critical erosion thresholds in the mud with eelgrass treatments (Fig. 3).

Belowground biomass was the only variable significantly correlated with less bed-load erosion in sandy sediment (Spearman, $r_s = -0.68$, $p < 0.001$) (Fig. 7a). None of the morphologic traits were significantly correlated with bed-load erosion. Eelgrass with lower percentage of mud seems to reduce less the bed-load

erosion compared to eelgrass with higher percentage of mud, although the correlation was not significant (Fig. 7b).

Discussion

This study showed that the bed-load erosion was reduced in sandy trials with eelgrass (either with leaves or only rhizomes and roots) compared with bare sediment, even at the highest wave velocities (≈ 27 cm s^{-1}). Nevertheless, turbidity increased in the presence of natural eelgrass or mimics compared to bare sediment at orbital velocities above 5 cm s^{-1} and 10 cm s^{-1} in both muddy and sandy sediments, respectively. Sediment properties showed key differences in the maximum turbidity reached with mud (≈ 272 mg L^{-1}) and with sand (≈ 74 mg L^{-1}) and the type of erosion (i.e., suspended load with mud vs. bed load with sand).

Eelgrass presence on sediment resuspension

Previous studies show that seagrass can reduce sediment resuspension by a reduction of the water flow and the shear stress compared to the unvegetated areas, either with currents (Gambi et al. 1990; Widdows et al. 2008) or waves (Ward et al. 1984; Hansen and Reidenbach 2012; Infantes et al. 2012; Ros et al. 2014). Nevertheless, the results of this study showed that eelgrass enhanced the resuspension of the sediment and lowered the critical erosion threshold both in sandy and muddy trials. Hydrodynamics inside the eelgrass patch could not be measured due to the small size (0.12 m^2, 35 × 35 cm^2). Other experiments with patches ranging from 2.2 to 0.3 m width have shown to increase the sediment dynamics created by the turbulence generated by the shoots or by the meadow edges under both currents (Fonseca and Koehl 2006; Bouma et al. 2007; Chen et al. 2012) and waves (Granata et al. 2001). Low plant densities could also increase the turbulence and scouring around shoots as flow moves through the sparse canopy (Bouma et al. 2009*a,b*; Lefebvre et al. 2010). This increase in turbulence and

scouring by the eelgrass presence suggests the observed increase in sediment resuspension and turbidity in all trials.

Sediment characteristics on turbidity and light attenuation

The comparison between muddy and sandy trials indicates that the critical erosion threshold and the subsequent increase in turbidity and light attenuation (K_d) are dependent on the sediment properties, in accordance with Bale et al. (2006), together with the interaction with eelgrass presence. In our experimental setup with a water depth of 25 cm, only the muddy sediment reduced the light below the minimum 20%, assessed for *Z. marina* (Dennison et al. 1993). Sandy treatments led to a major part of erosion in the form of bed load (from 2567 to 918 g) and a small part as suspended load (from 154 to 329 g), not causing high turbidity nor light reduction, in agreement with Houwing (1999). In contrast, muddy sediment with mean grain size smaller than 62.5 μm passed directly to suspended load with negligible bed-load phase, causing higher turbidity and light reduction (Widdows et al. 2008; Grabowski et al. 2011). The response was similar for mimic treatments, although mimics needed less wave velocities to reduce the percentage of light than natural eelgrass (10 cm s^{-1} and 15 cm s^{-1}, respectively). Mimic shoots were slightly stiffer than natural eelgrass, which is related with more scouring and turbulences around the shoots (Bouma et al. 2009*b*; Ros et al. 2014).

Importance of the belowground biomass: Applications for conservation and restoration

Bed-load erosion of sandy sediment was reduced in treatments with eelgrass compared to bare sediment. Furthermore, there were no differences between the treatments of full canopy eelgrass (aboveground and belowground biomass), and only roots and rhizomes (only belowground biomass), suggesting that the effect of sediment stabilization is mediated by the belowground biomass rather than the canopy. These results are important and in line with earlier findings from Christianen et al. (2013), which increases the still limited available literature on this topic. In this study, eelgrass present in sandy sediment had a dense network of roots and rhizomes with root length densities of 0.8 cm cm^{-3}. In terrestrial plants, a high density of roots with < 1 mm of diameter is related with less erosion (Baets et al. 2009). In contrast, eelgrass in muddy sediment with root length density of 0.003 cm cm^{-3} led to less aggregation and retention of the sediment, as found by Widdows et al. (2008). In addition, the sediment properties of sandy eelgrass samples with higher percentage mud (> 20%) might have increased the sediment cohesiveness reducing even more the erodibility (Brown et al. 1995; Gailani et al. 2001) (Fig. 7b). Nevertheless, eelgrass samples with less mud (< 5%) still had less bed-load erosion than the bare sediment (with higher percentage of mud) (Fig. 7b), suggesting again that belowground biomass may play a major role reducing bed-load erosion.

This study underlines the importance of the conservation of the existent eelgrass meadows with developed belowground biomass to reduce the sediment erosion by bed-load transport. The data obtained in this study confirm that an eelgrass patch of 0.12 m^2 with developed belowground biomass has a stabilizing effect of the sediment, reducing bed-load transport. On the other hand, such a small patch will not have any effect preventing resuspension of the sediment. This experiment provides more evidence that the fragmentation of the meadows due to anthropogenic causes could increase the turbidity by exposing more edges of the meadow to hydrodynamics, which increases the sediment resuspension (El Allaoui et al. 2016).

Sediment characteristics such as bulk density and grain size, exposure to hydrodynamics, and patch size are important factors to consider during eelgrass restoration. Our results suggest that in sites with sediment median grain size smaller than 75 μm and exposure to orbital velocities above 10 cm s^{-1}, sediment resuspension may be a problem in the restorations (Van Der Heide et al. 2007; Moksnes et al. 2018), and larger patches than 0.12 m^2 might be needed to reduce sediment resuspension (Silliman et al. 2015; van Katwijk et al. 2016). On the other hand, in sandy sediments with mean grain size larger than 130 μm and exposed to orbital velocities up to 30 cm s^{-1}, sediment resuspension might not reduce the light below the 20% in shallow waters (Adams et al. 2016). Bed-load erosion might however be the cause of restoration failure due to the lack of a developed network of roots and rhizomes and uprooting of the initial plant units. In this case, to start a self-reinforcing feedback with sediment stabilization and low bed-load erosion, wave barriers (Maxwell et al. 2017) or biodegradable geotextiles (Zanuttigh et al. 2015) could be implemented to reduce hydrodynamics and stabilize the sediment at the restoration site until the seagrass patches develop a dense root and rhizome network.

References

Aberle, J., V. Nikora, and R. Walters. 2004. Effects of bed material properties on cohesive sediment erosion. Mar. Geol. **207**: 83–93. doi:10.1016/j.margeo.2004.03.012

Adams, M. P., and others. 2016. Feedback between sediment and light for seagrass: Where is it important? Limnol. Oceanogr. **61**: 1937–1955. doi:10.1002/lno.10319

Amos, C. L., J. Grant, G. R. Daborn, and K. Black. 1992. Sea Carousel—a benthic, annular flume. Estuar. Coast. Shelf Sci. **34**: 557–577. doi:10.1016/S0272-7714(05)80062-9

Amos, C. L., T. Feeney, T. F. Sutherland, and J. L. Luternauer. 1997. The stability of fine-grained sediments from the Fraser River Delta. Estuar. Coast. Shelf Sci. **45**: 507–524. doi:10.1006/ecss.1996.0193

Baets, S., J. Poesen, A. Knapen, and P. Galindo. 2009. Impact of root architecture on the erosion-reducing potential of roots during concentrated flow. Earth Surf. Process. Landf. **34**: 155–161. doi:10.1002/esp

Bale, A. J., J. Widdows, C. B. Harris, and J. A. Stephens. 2006. Measurements of the critical erosion threshold of surface sediments

along the Tamar Estuary using a mini-annular flume. Cont. Shelf Res. **26**: 1206–1216. doi:10.1016/j.csr.2006.04.003

Beer, S., M. Björk, and J. Beardall. 2014. Photosynthesis in the marine environment, Wiley-Blackwell.

Bos, A. R., T. J. Bouma, G. L. J. de Kort, and M. M. van Katwijk. 2007. Ecosystem engineering by annual intertidal seagrass beds: Sediment accretion and modification. Estuar. Coast. Shelf Sci. **74**: 344–348. doi:10.1016/j.ecss.2007.04.006

Bouma, T. J., L. A. van Duren, S. Temmerman, T. Claverie, A. Blanco-Garcia, T. Ysebaert, and P. M. J. Herman. 2007. Spatial flow and sedimentation patterns within patches of epibenthic structures: Combining field, flume and modelling experiments. Cont. Shelf Res. **27**: 1020–1045. doi:10.1016/j.csr.2005.12.019

Bouma, T. J., M. Friedrichs, B. K. Van Wesenbeeck, S. Temmerman, G. Graf, and P. M. J. Herman. 2009*a*. Density-dependent linkage of scale-dependent feedbacks: A flume study on the intertidal macrophyte *Spartina anglica*. Oikos **118**: 260–268. doi:10.1111/j.1600-0706.2008.16892.x

Bouma, T. J., and others. 2009*b*. Effects of shoot stiffness, shoot size and current velocity on scouring sediment from around seedlings and propagules. Mar. Ecol. Prog. Ser. **388**: 293–297. doi:10.3354/meps08130

Bouma, T. J., and others. 2014. Identifying knowledge gaps hampering application of intertidal habitats in coastal protection: Opportunities & steps to take. Coast. Eng. **87**: 147–157. doi:10.1016/j.coastaleng.2013.11.014

Brown, J., A. Colling, D. Park, J. Phillips, D. Rothery, and J. Wright. 1995. An introduction to shallow-water environments and their sediments, p. 72–94. *In* G. Bearman [ed.], Waves, tides and shallow-water processes. The Open Univ.

Chen, S. C., H. C. Chan, and Y. H. Li. 2012. Observations on flow and local scour around submerged flexible vegetation. Adv. Water Resour. **43**: 28–37. doi:10.1016/j.advwatres.2012.03.017

Christianen, M. J. A., J. van Belzen, P. M. J. Herman, M. M. van Katwijk, L. P. M. Lamers, P. J. M. van Leent, and T. J. Bouma. 2013. Low-canopy seagrass beds still provide important coastal protection services. PLoS One **8**: e62413. doi:10.1371/journal.pone.0062413

Dahl, M., E. Infantes, R. Clevesjö, H. W. Linderholm, M. Björk, and M. Gullström. 2018. Increased current flow enhances the risk of organic carbon loss from *Zostera marina* sediments: Insights from a flume experiment. Limnol. Oceanogr. **63**: 2793–2805. doi:10.1002/lno.11009

Dennison, W. C. 1987. Effects of light on seagrass photosynthesis, growth and depth distribution. Aquat. Bot. **27**: 15–26. doi:10.1016/0304-3770(87)90083-0

Dennison, W. C., R. J. Orth, K. A. Moore, J. C. Stevenson, V. Carter, S. Kollar, P. W. Bergstrom, and R. A. Batiuk. 1993. Assessing water quality with submersed aquatic vegetation habitat requirements as barometers of Chesapeake Bay health. Bioscience **43**: 86–94. doi:10.2307/1311969

Duarte, C. M. 1991. Seagrass depth limits. Aquat. Bot. **40**: 363–377. doi:10.1016/0304-3770(91)90081-F

Einstein, H. A., A. G. Anderson, and J. W. Johnson. 1940. A distinction between bed-load and suspended load in natural streams. Eos Trans. AGU **21**: 628–633. doi:10.1029/TR021i002p00628

El Allaoui, N., T. Serra, J. Colomer, M. Soler, X. Casamitjana, and C. Oldham. 2016. Interactions between fragmented seagrass canopies and the local hydrodynamics. PLoS One **11**: e0156264. doi:10.1371/journal.pone.0156264

Feagin, R. A., S. M. Lozada-Bernard, T. M. Ravens, I. Mo, K. M. Yeager, and A. H. Baird. 2009. Does vegetation prevent wave erosion of salt marsh edges? Proc. Natl. Acad. Sci. USA **106**: 10109–10113. doi:10.1073/pnas.0901297106

Fonseca, M. S., and M. A. R. Koehl. 2006. Flow in seagrass canopies: The influence of patch width. Estuar. Coast. Shelf Sci. **67**: 1–9. doi:10.1016/j.ecss.2005.09.018

Gailani, J. Z., L. Jin, J. McNeil, and W. Lick. 2001. Effects of bentonite clay on sediment erosion rates. DOER technical notes collection (ERDC TN-DOER-N9). U.S. Army Engineer Research and Development Center.

Gambi, M. C., A. R. M. Nowell, and P. A. Jumars. 1990. Flume observations on flow dynamics in *Zostera marina* (eelgrass) beds. Mar. Ecol. Prog. Ser. **61**: 159–169. doi:10.3354/meps061159

Ganthy, F., L. Soissons, P. G. Sauriau, R. Verney, and A. Sottolichio. 2015. Effects of short flexible seagrass *Zostera noltei* on flow, erosion and deposition processes determined using flume experiments. Sedimentology **62**: 997–1023. doi:10.1111/sed.12170

Gedan, K. B., B. R. Silliman, and M. D. Bertness. 2009. Centuries of human-driven change in salt marsh ecosystems. Ann. Rev. Mar. Sci. **1**: 117–141. doi:10.1146/annurev.marine.010908.163930

González-Ortiz, V., L. G. Egea, R. Jimeńez-Ramos, F. Moreno-Marín, J. L. Pérez-Lloréns, T. J. Bouma, and F. G. Brun. 2014. Interactions between seagrass complexity, hydrodynamic flow and biomixing alter food availability for associated filter-feeding organisms. PLoS One **9**: e104949. doi:10.1371/journal.pone.0104949

Grabowski, R. C., I. G. Droppo, and G. Wharton. 2011. Earth-science reviews erodibility of cohesive sediment: The importance of sediment properties. Earth Sci. Rev. **105**: 101–120. doi:10.1016/j.earscirev.2011.01.008

Gracia, A., N. Rangel-Buitrago, J. A. Oakley, and A. T. Williams. 2018. Use of ecosystems in coastal erosion management. Ocean Coast. Manag. **156**: 277–289. doi:10.1016/j.ocecoaman.2017.07.009

Granata, T. C., T. Serra, J. Colomer, X. Casamitjana, C. M. Duarte, and E. Gacia. 2001. Flow and particle distributions in a nearshore seagrass meadow before and after a storm. Mar. Ecol. Prog. Ser. **218**: 95–106. doi:10.3354/meps218095

Hansen, J. C. R., and M. A. Reidenbach. 2012. Wave and tidally driven flows in eelgrass beds and their effect on sediment suspension. Mar. Ecol. Prog. Ser. **448**: 271–287. doi:10.3354/meps09225

Houwing, E. J. J. 1999. Determination of the critical erosion threshold of cohesive sediments on intertidal mudflats along the Dutch Wadden Sea coast. Esuar. Coast. Shelf Sci. **49**: 545–555. doi:10.1006/ecss.1999.0518

Infantes, E., A. Orfila, G. Simarro, J. Terrados, M. Luhar, and H. Nepf. 2012. Effect of a seagrass (*Posidonia oceanica*) meadow on wave propagation. Mar. Ecol. Prog. Ser. **456**: 63–72. doi:10.3354/meps09754

La Nafie, Y. A., C. B. de los Santos, F. G. Brun, M. M. van Katwijk, and T. J. Bouma. 2012. Waves and high nutrient loads jointly decrease survival and separately affect morphological and biomechanical properties in the seagrass *Zostera noltii*. Limnol. Oceanogr. **57**: 1664–1672. doi:10.4319/lo.2012.57.6.1664

Lefebvre, A., C. E. L. Thompson, and C. L. Amos. 2010. Influence of *Zostera marina* canopies on unidirectional flow, hydraulic roughness and sediment movement. Cont. Shelf Res. **30**: 1783–1794. doi:10.1016/j.csr.2010.08.006

Lo, V. B., T. J. Bouma, J. van Belzen, C. Van Colen, and L. Airoldi. 2017. Interactive effects of vegetation and sediment properties on erosion of salt marshes in the Northern Adriatic Sea. Mar. Environ. Res. **131**: 32–42. doi:10.1016/j.marenvres.2017.09.006

Maxwell, P. S., and others. 2017. The fundamental role of ecological feedback mechanisms for the adaptive management of seagrass ecosystems – a review. Biol. Rev. **92**: 1521–1538. doi:10.1111/brv.12294

McLeod, E., and others. 2011. A blueprint for blue carbon: Toward an improved understanding of the role of vegetated coastal habitats in sequestering CO_2. Front. Ecol. Environ. **9**: 552–560. doi:10.1890/110004

Menéndez, M., and P. L. Woodworth. 2010. Changes in extreme high water levels based on a quasi-global tide-gauge data set. J. Geophys. Res. Oceans **115**: 1–15. doi:10.1029/2009JC005997

Moksnes, P. O., L. Eriander, E. Infantes, and M. Holmer. 2018. Local regime shifts prevent natural recovery and restoration of lost eelgrass beds along the Swedish West Coast. Estuaries Coast. **1**: 1712–1731. doi:10.1007/s12237-018-0382-y

Möller, I., and others. 2014. Wave attenuation over coastal salt marshes under storm surge conditions. Nat. Geosci. **7**: 727–731. doi:10.1038/ngeo2251

Narayan, S., and others. 2016. The effectiveness, costs and coastal protection benefits of natural and nature-based defences. PLoS One **11**: 1–18. doi:10.1371/journal.pone.0154735

Orth, R. J., and others. 2006. A global crisis for seagrass ecosystems. Bioscience **56**: 987–996. doi:10.1641/0006-3568(2006)56[987:AGCFSE]2.0.CO;2

Ros, À., J. Colomer, T. Serra, D. Pujol, M. Soler, and X. Casamitjana. 2014. Experimental observations on sediment resuspension within submerged model canopies under oscillatory flow. Cont. Shelf Res. **91**: 220–231. doi:10.1016/j.csr.2014.10.004

Silliman, B. R., and others. 2015. Facilitation shifts paradigms and can amplify coastal restoration efforts. Proc. Natl. Acad. Sci. USA **112**: 14295–14300. doi:10.1073/pnas.1515297112

Spencer, T., and others. 2016. Salt marsh surface survives true-to-scale simulated storm surges. Earth Surf. Process. Landf. **41**: 543–552. doi:10.1002/esp.3867

Temmerman, S., P. Meire, T. J. Bouma, P. M. J. Herman, T. Ysebaert, and H. J. De Vriend. 2013. Ecosystem-based coastal defence in the face of global change. Nature **504**: 79–83. doi:10.1038/nature12859

Van Der Heide, T., E. H. Van Nes, G. W. Geerling, A. J. P. Smolders, T. J. Bouma, and M. M. Van Katwijk. 2007. Positive feedbacks in seagrass ecosystems: Implications for success in conservation and restoration. Ecosystems **10**: 1311–1322. doi:10.1007/s10021-007-9099-7

van Katwijk, M. M., and others. 2016. Global analysis of seagrass restoration: The importance of large-scale planting. J. Appl. Ecol. **53**: 567–578. doi:10.1111/1365-2664.12562

Vousdoukas, M. I., L. Mentaschi, E. Voukouvalas, M. Verlaan, S. Jevrejeva, L. P. Jackson, and L. Feyen. 2018. Global probabilistic projections of extreme sea levels show intensification of coastal flood hazard. Nat. Commun. **9**: 2360. doi:10.1038/s41467-018-04692-w

Wang, H., and others. 2017. Zooming in and out: Scale-dependence of extrinsic and intrinsic factors affecting salt marsh erosion. J. Geophys. Res. Earth Surf. **112**:1455–1470. doi:10.1002/2016JF004193

Ward, L. G., W. Michael Kemp, and W. R. Boynton. 1984. The influence of waves and seagrass communities on suspended particulates in an estuarine embayment. Mar. Geol. **59**: 85–103. doi:10.1016/0025-3227(84)90089-6

Widdows, J., N. D. Pope, M. D. Brinsley, H. Asmus, and R. M. Asmus. 2008. Effects of seagrass beds (*Zostera noltii* and *Z. marina*) on near-bed hydrodynamics and sediment resuspension. Mar. Ecol. Prog. Ser. **358**: 125–136. doi:10.3354/meps07338

Zanuttigh, B., R. Nicholls, R. Thompson, J.-P. Vanderlinden, and H. Burcharth. 2015. Coastal risk management in a changing climate. Elsevier.

Conflict of Interest

None declared.